

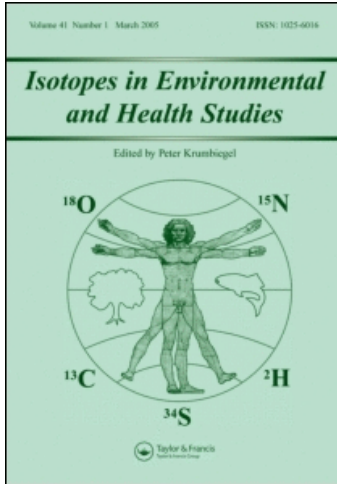
This article was downloaded by: [Canadian Research Knowledge Network]

On: 7 January 2011

Access details: Access Details: [subscription number 918588849]

Publisher Taylor & Francis

Informa Ltd Registered in England and Wales Registered Number: 1072954 Registered office: Mortimer House, 37-41 Mortimer Street, London W1T 3JH, UK



Isotopes in Environmental and Health Studies

Publication details, including instructions for authors and subscription information:

<http://www.informaworld.com/smpp/title~content=t713643233>

Stable isotopic and geochemical variability within shallow groundwater beneath a hardwood hammock and surface water in an adjoining slough (Everglades National Park, Florida, USA)

Lee J. Florea^a; Dorien K. McGee^b

^a Department of Geography and Geology, Western Kentucky University, Bowling Green, KY, USA ^b Department of Geology, University of South Florida, Tampa, FL, USA

Online publication date: 23 June 2010

To cite this Article Florea, Lee J. and McGee, Dorien K.(2010) 'Stable isotopic and geochemical variability within shallow groundwater beneath a hardwood hammock and surface water in an adjoining slough (Everglades National Park, Florida, USA)', *Isotopes in Environmental and Health Studies*, 46: 2, 190 – 209

To link to this Article: DOI: 10.1080/10256016.2010.494770

URL: <http://dx.doi.org/10.1080/10256016.2010.494770>

PLEASE SCROLL DOWN FOR ARTICLE

Full terms and conditions of use: <http://www.informaworld.com/terms-and-conditions-of-access.pdf>

This article may be used for research, teaching and private study purposes. Any substantial or systematic reproduction, re-distribution, re-selling, loan or sub-licensing, systematic supply or distribution in any form to anyone is expressly forbidden.

The publisher does not give any warranty express or implied or make any representation that the contents will be complete or accurate or up to date. The accuracy of any instructions, formulae and drug doses should be independently verified with primary sources. The publisher shall not be liable for any loss, actions, claims, proceedings, demand or costs or damages whatsoever or howsoever caused arising directly or indirectly in connection with or arising out of the use of this material.

Stable isotopic and geochemical variability within shallow groundwater beneath a hardwood hammock and surface water in an adjoining slough (Everglades National Park, Florida, USA)

Lee J. Florea^{a*} and Dorien K. McGee^b

^a*Department of Geography and Geology, Western Kentucky University, 1906 College Heights Blvd., Bowling Green, KY 42101, USA;* ^b*Department of Geology, University of South Florida, 4202 E. Fowler Ave. SCA 528, Tampa, FL 33620, USA*

(Received 8 January 2010; final version received 12 May 2010)

Data from a 10-month monitoring study during 2007 in the Everglades ecosystem provide insight into the variation of $\delta^{18}\text{O}$, δD , and ion chemistry in surface water and shallow groundwater. Surface waters are sensitive to dilution from rainfall and input from external sources. Shallow groundwater, on the other hand, remains geochemically stable during the year. Surface water input from canals derived from draining agricultural areas to the north and east of the Everglades is evident in the ion data. $\delta^{18}\text{O}$ and δD values in shallow groundwater remain near the mean of -2.4 and -12 ‰, respectively. ^{18}O and D values are enriched in surface water compared with shallow groundwater and fluctuate in sync with those measured in rainfall. The local meteoric water line (LMWL) for precipitation is in close agreement with the global meteoric water line; however, the local evaporation line (LEL) for surface water and shallow groundwater is $\delta\text{D} = 5.6 \delta^{18}\text{O} + 1.5$, a sign that these waters have experienced evaporation. The intercept of the LMWL and LEL indicates that the primary recharge to the Everglades is tropical cyclones or fronts. δ deuterium to $\delta^{18}\text{O}$ excess (D_{ex} values) generally reveal two moisture sources for precipitation, a maritime source during the fall and winter ($D_{\text{ex}} > 10$ ‰) and a continental-influenced source ($D_{\text{ex}} < 10$ ‰) in the spring and summer.

Keywords: isotope ecology; hydrogen-2; oxygen-18; Everglades National Park; USA; δD to $\delta^{18}\text{O}$ excess; Everglades agricultural area; mid-summer drought

1. Introduction

Stable isotopes in natural waters have become a powerful tool for delineating transport pathways in ground water [1], surface water [2], atmospheric moisture [3], and the degree of interaction between these reservoirs [4]. Combined with basic water chemistry, time-series measurements of the stable isotopes of hydrogen (^1H and D) and the two most common stable isotopes of oxygen (^{16}O and ^{18}O) can also be a means to discriminate between the sources for surface water and atmospheric moisture [5]. Because stable isotopes of hydrogen and oxygen can help us to understand past and present patterns of climate [6,7], these same isotopes can help scientists better manage water resources, particularly in coastal regions with limited freshwater, such as

*Corresponding author. Email: lee.florea@wku.edu

small islands in the Bahamas with negative water budgets [8], or in regions with exceptional freshwater demand, such as the Biscayne aquifer of southeast Florida [9].

A drive to better understand the hydrologic processes operating within the Biscayne aquifer and Everglades National Park (ENP) govern the goals of this study and the larger goals of the Comprehensive Everglades Restoration Plan (CERP) as authorised by the US Congress in 2000. Over the 30-year lifespan of CERP, the state and federal governments will take major steps to improve how and when water enters the Everglades ecosystem. To that end, this paper provides insight into the impact of seasonal climate and shifting moisture sources upon stable isotopes of hydrogen and oxygen, basic water chemistry, and major ions in samples of precipitation, surface water, and shallow groundwater within one part of the Everglades ecosystem of south Florida. The data for this study come from water samples collected during a 10-month monitoring study in 2007 at three sites in the eastern part of ENP: Palma Vista Cave (PVC), a small cave within Palma Vista Hammock; a shallow well in the bedrock within Palma Vista Hammock; and Taylor Slough (TS) to the east of Palma Vista Hammock (Figure 1).

1.1. Stable isotopic processes

Liquid water or water vapour within a natural ecosystem contains proportions of the stable isotopes of hydrogen and oxygen relative to the processes that move water into the environment. The isotopic signature of water is commonly reported in the standard δ -notation:

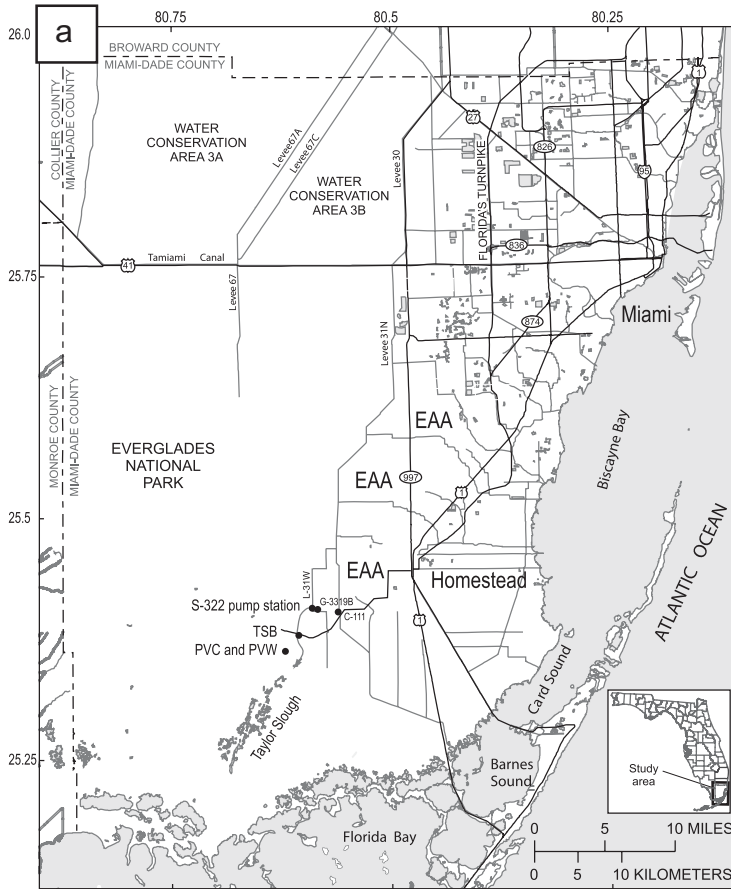
$$\delta = \left(\frac{R_{\text{sample}}}{R_{\text{standard}}} - 1 \right) \times 1000,$$

where R is the ratio of heavy to light isotope. Fractionation of oxygen and hydrogen from a reservoir of water produces values of δD and $\delta^{18}\text{O}$ that follow the Rayleigh Law,

$$\delta_f = \delta_0 - \varepsilon^* \cdot \log f,$$

where ε^* is the equilibrium fractionation factor, f is the fraction of water remaining in the system ($0 < f < 1$), and δ_0 and δ_f are the isotopic signatures of the water before and after fractionation, respectively. In precipitation formed in equilibrium with atmospheric water vapour at a certain temperature and disconnected from the moisture source, the degree of Rayleigh distillation during the cloud rainout depends largely upon: source and event latitude, altitude of condensation, and the amount and duration of precipitation events [1–3,10–15]. In fact, these factors control the global variation of δD versus $\delta^{18}\text{O}$, which gives the global meteoric water line (GMWL) equation: $\delta\text{D} = 8(\delta^{18}\text{O}) + 10$ [5]. The degree of influence of each process of the Rayleigh distillation depends largely on local patterns of climate. Air masses that mix produce a blending of the isotopic signatures of each air mass [3].

Climate-driven fractionation processes create additional variation in the ratio of hydrogen to oxygen isotope during evaporation, and these processes potentially produce deviations from the GMWL [2,4,16]. Waters that undergo significant evaporation during or after rainfall will be enriched in the heavier isotopes, and the enrichment of D is greater than the enrichment of ^{18}O in the remaining liquid as relative humidity (RH) increases [3]. The effect of evaporation upon the stable isotopes is often quantified using the equation $D_{\text{ex}} = \delta\text{D} - (8 \times \delta^{18}\text{O})$, which calculates the excess of D to ^{18}O from that predicted by the GMWL [3,17]. According to Dansgaard [3], D_{ex} can be calculated for a composite sample of precipitation as the y-intercept for a line with a forced slope of 8 that passes through the values of δD and $\delta^{18}\text{O}$. The slope of 8 is used because it is the slope of the GMWL and results from the fact that the global average water vapour forms from an average humidity of about 85% over the oceans. Similarly, D_{ex} can be



Base from U.S. Geological Survey digital data, 1972
 Universal Transverse Mercator projection, Zone 17, Datum NAD 83

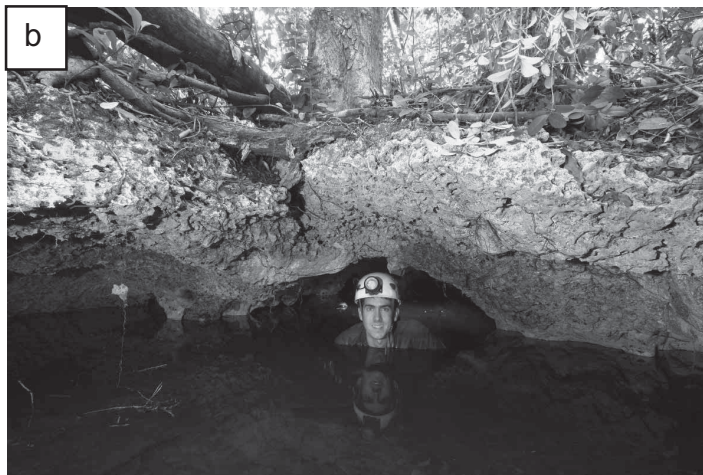


Figure 1. (a) Study area in ENP in southeast Florida with Taylor Slough (TS) labelled (grey areas are open water bodies). TS has its origin at the S-322 pumping station on the L-31W canal. Both sampling stations are identified: TS Bridge (TS – NWIS ID 252404080362401) and PVC and PVW (NWIS ID 252312080371901). Sampling stations C-111 and G-3319B are used for comparison of water chemistry. (Figure 1a modified from Figure 1 of Cunningham *et al.* [18].) (b) Brian Killingbeck in the entrance to PVC within a hardwood hammock that adjoins TS (photo by Alan Cressler). Note the thin vadose zone and the touching-vug macropores in the bedrock of the hammock.

computed as the y -intercept of a regression through a collection of samples. Assuming no additional input of moisture, precipitation following the GMWL during rainout will preserve a D_{ex} value of 10. Deviations from this y -intercept are an indication of additional sources of moisture [3,19,20].

D_{ex} for a single point has a potential associated analytical error; however, comparing values between two precipitation samples gives information about the RH that produced those samples [3,16–19]. Whereas values of D_{ex} below 10 indicate evaporation from a source more humid than the global ocean average, values of D_{ex} above 10 are commonly interpreted as resulting from cooler and dryer air masses [17]. In a recent example from the Tibet Plateau in China, for example, values of D_{ex} changed according to the monsoon [21]. In the summer, values of D_{ex} were lower because of warm, moist air migrating north from the Indian Ocean. Values of D_{ex} in the winter, in contrast, were higher as sources of moisture were derived from continental sources [21].

Furthermore, precipitation derived from evaporation will have greater D_{ex} than that derived from transpiration-based moisture sources because there is no fractionation of soil water during transpiration [22]. Farquhar *et al.* [23], in particular, review δD and $\delta^{18}\text{O}$ values in plant physiology and note that ‘leaf transpiration contributes water vapour to the atmosphere, with an oxygen isotope composition equal to that of soil water. Similarly, the evaporation of rain intercepted by the leaves involves no fractionation when all the water has been evaporated’ [23, p. 16]. Therefore, samples grouped in a meaningful way can be used to give a weighted average D_{ex} that provides information about the average RH and influence of transpiration upon that group of waters.

The effects of evaporation and transpiration on D_{ex} are therefore expected in regions with a strongly seasonal climate, such as the tropical, dry winter (Aw) and the tropical, monsoonal (Am) regions in the Köppen classification system [24] governed by the position of the Intertropical Convergence Zone (ITCZ). In the Northern Hemisphere, dry winters and summer monsoons impact broad regions of Southeast Asia and India, sub-Saharan Africa, and the circum Caribbean including the focus of this paper, the Everglades ecosystem of south Florida.

1.2. The mid-summer drought

Rainfall throughout the Caribbean, including the Everglades, is strongly seasonal; some maps of the Köppen classification depict south Florida as a tropical, dry winter climate [25]. Others further subdivide the southeast coast of Florida, a tropical, monsoonal climate, where easterly long waves of geostrophic flow entrained within the Trade Winds convey seasonal moisture evaporated from the Gulf Stream [26].

The rainfall regimen in the coastal regions of the Caribbean region, such as in south Florida, is dominated by frequent, and often intense, convection storms during the summer months and less frequent tropical cyclones during the late summer and early fall. Interestingly, typical annual hyetographs in the circum-Caribbean also reveal a mid-summer period of reduced rainfall often referred to as the mid-summer drought (MSD) [27–29]. While several climatologic models have been proposed for the MSD [30–32], this pervasive phenomena is thought, at least in the central Caribbean, to be the product of an increase in surface pressure caused by a change in wind field dominated by the Westerlies in the early summer to the Trade Winds in the late summer as the ITCZ migrates to its furthest northerly position [33]. Gamble *et al.* [34] demonstrate that the progression of the MSD is from east to west, appearing in the West Indies in May–June and diminishing during July–August in south Florida, Cuba, and Jamaica. Regardless of the cause or the timing, a strong MSD can intensify the stress on water resources in the circum-Caribbean.

2. The Everglades ecosystem

ENP encompasses 1.5 million acres of grassland glades, tropical hardwood hammocks, pine rocklands, cypress strands, and mangrove marshes. Subtle differences in elevation, salinity, and seasonal rainfall control the spatial distribution of these ecosystems. Of particular interest to this study are freshwater sloughs, often miles wide, which convey freshwater from Lake Okeechobee in the north to Florida Bay in the south, and the tropical hardwood hammocks in the east-central portion of ENP with exposed late-Pleistocene limestone. In particular, this study focusses on the central portions of TS and adjacent Palma Vista Hammock (Figure 1a).

2.1. Hydrogeologic overview

Palma Vista Hammock, other nearby tropical hardwood hammocks, and nearby pine rocklands comprise the southwestern limits of the Atlantic Coastal Ridge, a relatively high, but low-relief topographic feature in southeast Florida. Much of the coastal ridge has been drained via canalisation and urbanised in the past century; the relatively higher elevations now host the Greater-Miami metropolitan area and the large agricultural district surrounding the city of Homestead.

The bedrock of the study area is the late Pleistocene (marine isotope sub-stage (MIS) 5e) Miami Limestone. Lithologically, this unit is a pelloidal-algal grainstone that is porous, with a matrix permeability measured between $10^{-12.4}$ and $10^{-13.5}$ m², and localised touching-vug macropores created by the syn-depositional bioturbation by endobenthic organisms [35]. XRD analyses of four samples of the Miami Limestone in Palma Vista Hammock reveal a composition dominated by calcite with an average of 12 % by weight of aragonite and less than 1 % by weight of quartz.

The carbonate bedrock throughout the Everglades ecosystem is greatly modified by dissolution. In the pine rocklands and tropical hardwood hammocks, for example, solution pits and other epikarst features convey recharge to the water table. Shallow collapse features in these limestones provide access to small, horizontal caves situated at the average perennial water table [36,37] (Figure 1b). Access to water and development of soils in these collapse features make them analogous to the 'banana holes' of small carbonate islands [38].

In the slough adjacent to Palma Vista Hammock, the water table during the wet season resides above the mean land surface. Sawgrass prairies dominate, growing from a layer of peat that mantles a complex corrosion surface. This surface has considerable relief, perhaps as much as a metre. A light-red-stained caliche is pervasive on this surface, indicating exposure and soil development since the last sea-level fall at the end of MIS 5e. The peat, with an average permeability of $10^{-12.5}$ m², ranges in thickness from 0.2 to 2 m [39].

The magnitude of interaction between surface water and shallow groundwater in the Everglades has important management implications for the south Florida ecosystem and the Biscayne aquifer. Meyers *et al.* [40] and Wilcox [41] used $\delta^{18}\text{O}$ and δD to characterise the flow of shallow groundwater along the northern and eastern boundaries of ENP. Price and Swart [42] used $\delta^{18}\text{O}$, δD , and major ion chemistry to quantify the rates of exchange between surface waters in the sloughs and shallow groundwater. Using ratios of the mean chloride concentrations in precipitation and shallow groundwater, their results estimate rates of recharge between 2 and 12 cm/year with higher rates in the pine rocklands because of reduced evaporation, a lack of soil and caliche, and the presence of open voids in the vadose zone.

2.2. Meteorological overview

Moisture sources for precipitation in the Everglades come from four main sources: continental moisture brought primarily during the winter and spring months as occasional frontal systems

entrained in the prevailing Westerlies; convective moisture, locally derived, during the warm summer months; convective, maritime moisture brought onshore from nearby tropical waters during the summer; and tropical cyclones conveyed long distances from low latitudes during the late summer and fall along the Trade Winds [43] (Figure 2a).

Vast expanses of open water, lush vegetation, and warm subtropical conditions contribute to high rates of evapotranspiration (ET) in the Everglades. In fact, German [44] measured rates of ET that ranged between 108 cm/year at a site where the water level is below the land surface and 146 cm/year at a site with exposed water and no emergent vegetation. This second number translates to more than 75 % of the average annual precipitation.

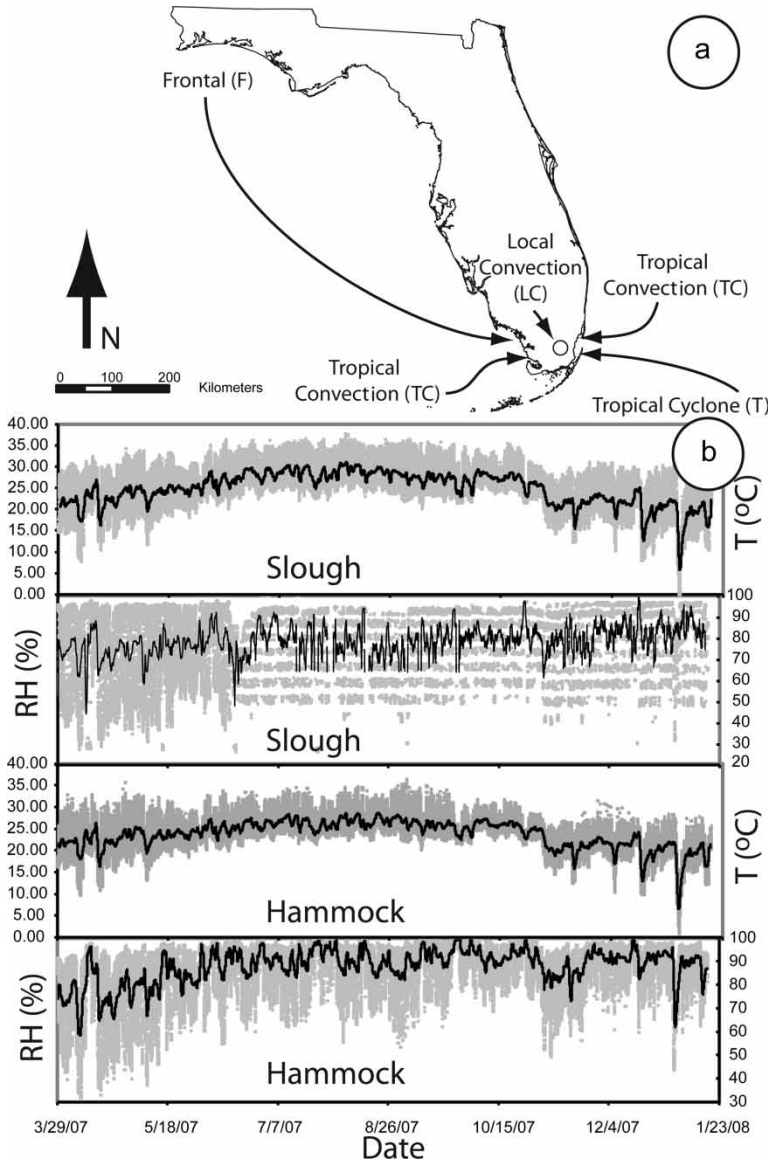


Figure 2. (a) Regional map of the Florida Peninsula with arrows that indicate the principle sources of precipitation. The open circle marks the approximate location of the field site. (b) Plots of temperature (T) and RH at TS and Palma Vista Hammock. The grey points mark the original data every 10 min. The solid black line represents a one-day moving average of the data. Gaps in the RH data at the slough are the result of probe failure at certain voltage ranges.

Temperature and RH measurements collected every 10 minutes during the course of this study at TS and Palma Vista Hammock reveal diurnal and seasonal patterns consistent with the intensity of solar insolation (Figure 2b). The temperature in TS is, on average, warmer than in Palma Vista Hammock, 24.7 °C (−0.2–37.8 °C, min–max) compared with 23.6 °C (0.9–36.5 °C, min–max), respectively. In contrast, the thick canopy of vegetation in the hammock maintains higher levels of RH than the slough, 87.8 % (32.0–99.7 %, min–max) compared with 74.9 % (1.9–100 %, min–max), respectively. Since sloughs, marl prairies, and sawgrass marshes are the dominant ecosystems in the Everglades, measurements of temperature and RH in TS are representative of mean annual conditions in southeast Florida. At an average RH of 75 % in southeast Florida, the theoretical slope of the relationship between δD versus $\delta^{18}O$ of evaporated waters should be between 5 and 6 [22]. This is validated by the long-term monitoring of surface waters in central Florida that show a local evaporation line (LEL) with a slope of 5.43 [2].

Furthermore, one could expect, using D_{ex} from precipitation, to differentiate between rainfall with moisture dominated by evaporation and moisture where transpiration comprises a significant component. Typically, D_{ex} of precipitation in temperate climates averages +10 ‰ [2]. In a west-central Florida example, Onac *et al.* [45] found $D_{ex} > 10$ ‰ during summer rainfall, which they attribute solely to greater evaporation. We propose that the variation of D_{ex} in TS and the eastern Everglades may vary according to wind patterns. Whereas the Westerlies from the late winter until the MSD could bring terrestrial-derived, and thus transpiration-influenced, moisture from the west and northwest, the Trade Winds after the MSD through the early winter might bring maritime-derived, and thus exclusively evaporation-based, moisture from the Bahamas and the Straits of Florida (Figure 1a).

3. Samples and analyses

The data comprise 22 sets of water samples collected every two weeks beginning on 29 March 2007 and ending on 16 January 2008. Each set consists of samples from: (1) precipitation (P); (2) surface waters collected at the USGS gauging station at the bridge over TS (National Water Information System (NWIS) station ID 252404080362401); (3) water within (PVC); and (4) water drawn from the nearby shallow well (PVW) in Palma Vista Hammock (both the cave and well share NWIS station ID 252312080371901). To supplement these samples, hourly water-level measurements were collected during the course of the study using piezometers at both the TS and PVW sites. Hourly measurements of precipitation amount were collected using a rain gauge at the TS site.

Precipitation was collected for analysis using a funnel and a 2 m length of 1 cm tygon tubing. The tubing was snugly inserted through a plastic seal and extended to the bottom of a plastic reservoir to minimise evaporation from the water surface in the reservoir back through the tube; the tubing and reservoir were shaded and shielded by aluminium foil and insulation to further reduce evaporation between sample collections. Samples of the precipitation were poured into a 60 ml glass bottle, sealed, and kept at 4 °C until the time of analysis for δD and $\delta^{18}O$. The remaining water in the collection reservoir was removed after each sample.

Surface waters from the slough, the well, and the cave were consistently drawn from 30 cm depth using a peristaltic pump. Three pore volumes were purged from the well prior to sample collection. The sample suite at each site presented in this paper include the following:

- (1) a sealed 60 ml glass bottle of filtered water collected for δD and $\delta^{18}O$ analyses;
- (2) a 125 ml opaque bottle of filtered water collected for nitrate analysis;
- (3) a 250 ml bottle of filtered water to analyse for dissolved major cations and anions;
- (4) a 250 ml bottle of filtered and acidified water to analyse for dissolved iron;

- (5) a 250 ml bottle of unfiltered water to analyse for suspended solids;
- (6) a 250 ml bottle of unfiltered and acidified water to analyse for total metals.

Additionally, during each sampling interval, we collected *in situ* measurements of pH, specific conductance (SpC), dissolved oxygen (DO), temperature, and total alkalinity at TS, PVC, and PVW. Two YSI datasondes were deployed during the period 18 September 2007 through 10 October 2007 to collect field parameters every 15 min; at TS, an OSM 600 collected SpC data, and at PVW, an OSM-600XLS collected temperature and pH in addition to SpC.

The majority of the geochemical analyses was conducted at the National Water Quality Lab in Denver, CO. These data are publically available from the NWIS database. Analyses of δD and $\delta^{18}\text{O}$ were conducted by the Reston Stable Isotope Lab (RSIL), Reston, VA, and reported with respect to the international VSMOW standard. The RSIL published precision for results is $\pm 1\%$ for δD and $\pm 0.1\%$ for $\delta^{18}\text{O}$.

4. Results

Figure 3 is a compilation of a hyetograph, water level data, and field measurements (temperature, pH, SpC, and DO). In the hyetograph, moisture sources (tropical wave, frontal system, local convection, tropical convection) are indicated for major events as well as the principle wind direction as identified from daily radar animations. The MSD is clearly present during mid- to late-August. In all cases, the surface water of the slough experiences the greatest geochemical variability, whereas the cave and well waters remain relatively stable and mutually similar.

Figure 4 is the shorter-term, higher-resolution data. In this data compilation, temperature, pH, and conductivity all respond to individual rain events, shown by an immediate increase in water level. These data also reveal daily variations in slough-water SpC that are an order of magnitude greater than at the cave and are due to solar insolation, diurnal fluctuations in water level from tidal forces or barometric fluctuations, and a sharp, temporary excursion in well-water SpC and pH during a precipitation event on the morning of 9/25 that contributed 3.5 cm of rainfall.

Figure 5 presents principle ion data in time-series format. There are similar trends in many of the parameters to those of the field measurements in Figure 3. As before, the slough waters experience the greatest excursions during the rainy season and the well and cave waters remain relatively stable throughout the year. There are, however, notable exceptions to this trend. For example, nitrate, sulphates, and potassium all display a pronounced excursion in the slough water sample on 4/11 that immediately follows the first major rainfall of the year (Figure 5). In another example, dissolved iron in the well water dramatically increases from 38 to 27 $\mu\text{g}/\text{l}$ at the beginning of the rainy season and remains above 200 $\mu\text{g}/\text{l}$ until after the start of the dry season. The dissolved iron in the cave water remains below 100 $\mu\text{g}/\text{l}$ except for an anomalously high spike of 290 $\mu\text{g}/\text{l}$ on 8/29 during the MSD (Figure 5). The charge balances are within 1.3% for this sample and less than 5% for all samples.

The values of δD and $\delta^{18}\text{O}$ in Figure 6 track each other for each of the three sites. Furthermore, the values of δD and $\delta^{18}\text{O}$ at the slough track the values for precipitation. Precipitation samples have the greatest variability with precipitation-weighted mean values of δD and $\delta^{18}\text{O}$ calculated at -17.5 and -3.4% , respectively. Values of δD and $\delta^{18}\text{O}$ from the slough water vary less than precipitation, but experience more fluctuation than either the well or the cave waters. The most depleted values of δD and $\delta^{18}\text{O}$ in precipitation and slough water occur following Tropical Storm Barry on 6/1 and 6/2 and following an unnamed tropical low on 9/25.

The mean values of δD (-1.3%) and $\delta^{18}\text{O}$ (-0.5%) in the slough water are more enriched in the heavier isotopes compared to the precipitation-weighted mean value of precipitation, indicating

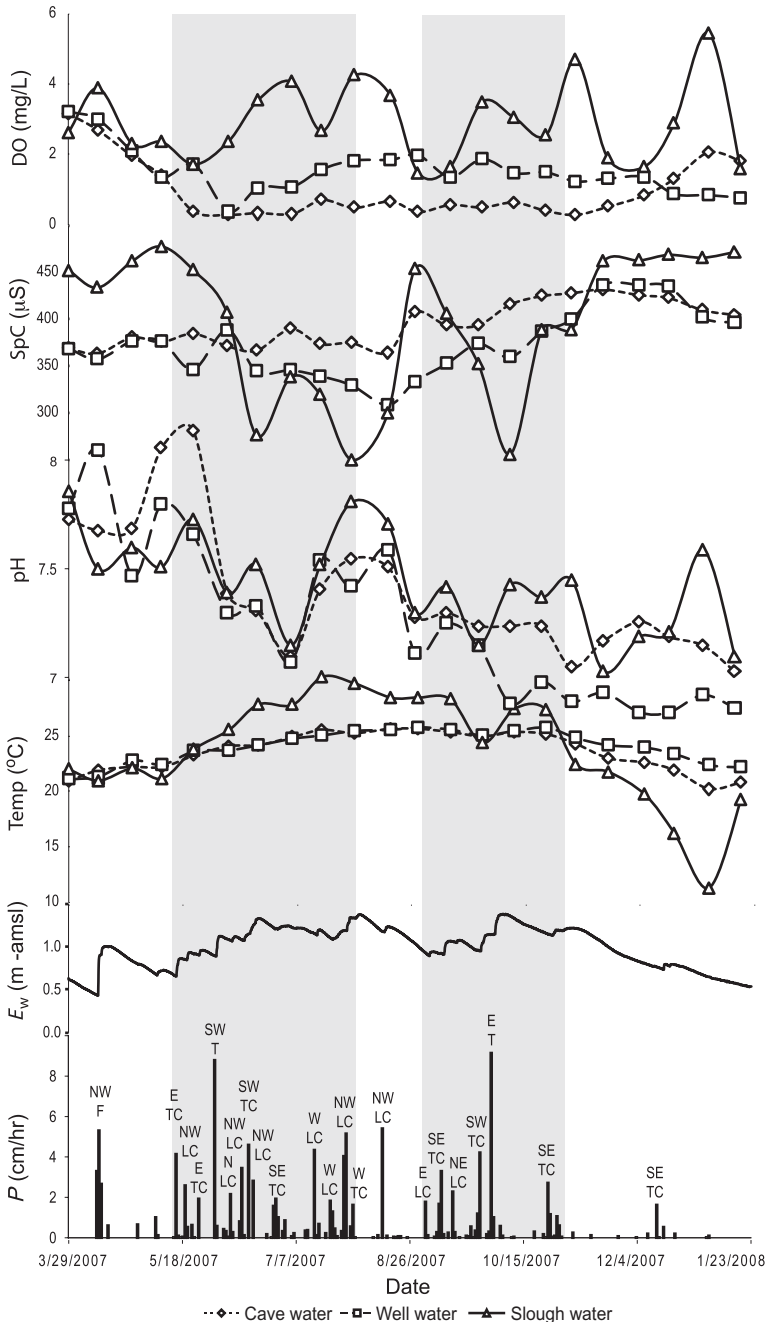


Figure 3. A compilation time-series plot of a hyetograph (P) and water level (E_w) data at TS, and field measurements of temperature (T), pH, SpC, and DO at all three sampling sites. Precipitation events that exceed a rate of 2 cm/h also include information about type and motion of the precipitation as indicated by Doppler radar (F – frontal, LC – local convection, TC – tropical convection, T – tropical storm or cyclone; N – north, NW – northwest, E – east, NE – northeast, S – south, SW – southwest, SE – southeast). Grey bars indicate the wet season.

a considerable effect of evaporation. δD and $\delta^{18}O$ values for the well (-11‰ , -2.2‰) and the cave (-12‰ , -2.4‰) are less than the slough and closer to the precipitation-weighted mean value of precipitation.

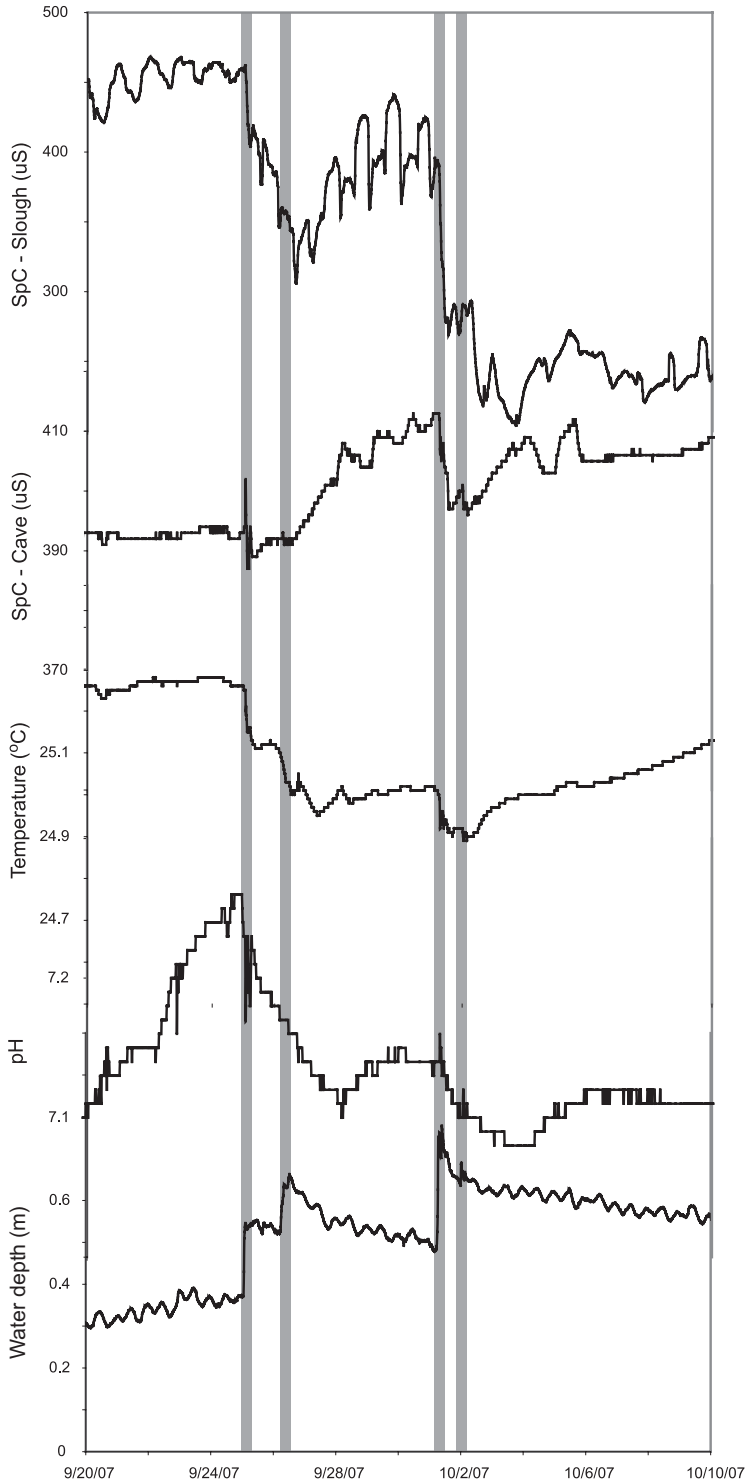


Figure 4. Shorter-term, higher-resolution data at PVC and TS that include water level at the cave, pH in the cave, temperature in the cave, SpC in both the cave and the slough. Grey bars indicate the occurrence of precipitation events.

Downloaded By: [Canadian Research Knowledge Network] At: 03:12 7 January 2011

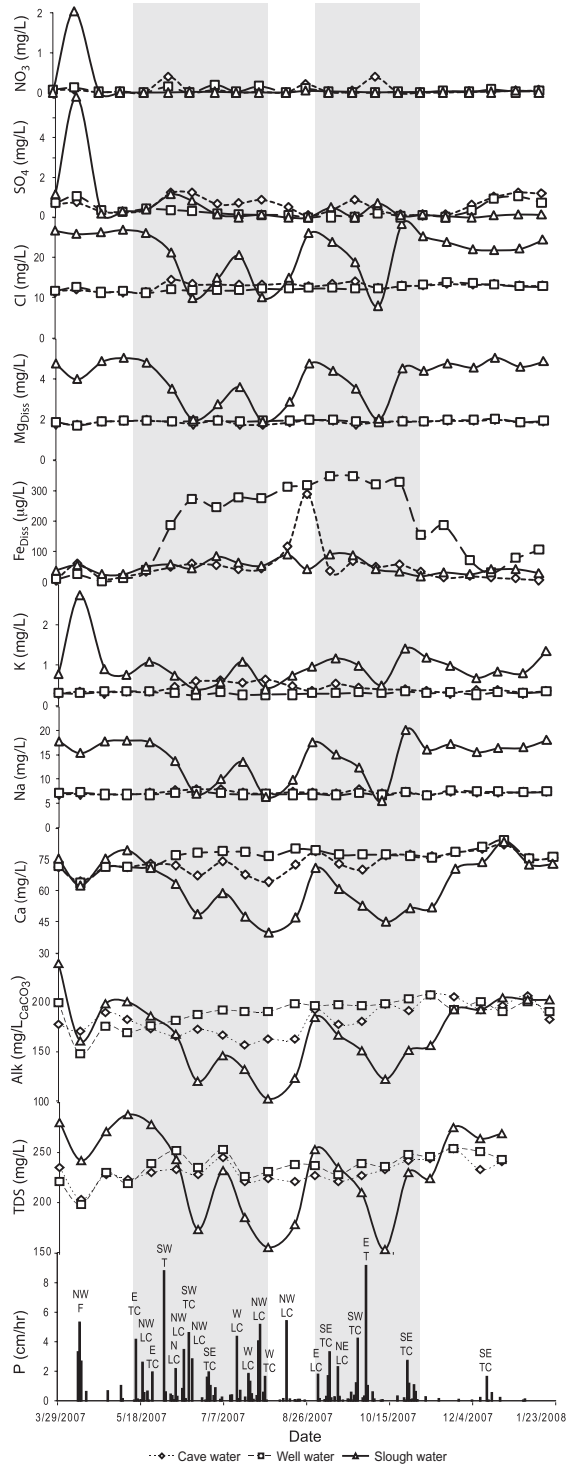


Figure 5. Compilation time-series plot of a hygograph (*P*), TDS, total alkalinity (Alk), major cations (Ca, Na, K, Fe, Mg), and major anions (Cl, SO₄, NO₃). Precipitation events that exceed a rate of 2 cm/h also include information about type and motion of the precipitation as indicated by Doppler radar (F – frontal, LC – local convection, TC – tropical convection, T – tropical storm or cyclone; N – north, NW – northwest, E – east, NE – northeast, S – south, SW – southwest, SE – southeast). Grey bars indicate the wet season.

Downloaded By: [Canadian Research Knowledge Network] At: 03:12 7 January 2011

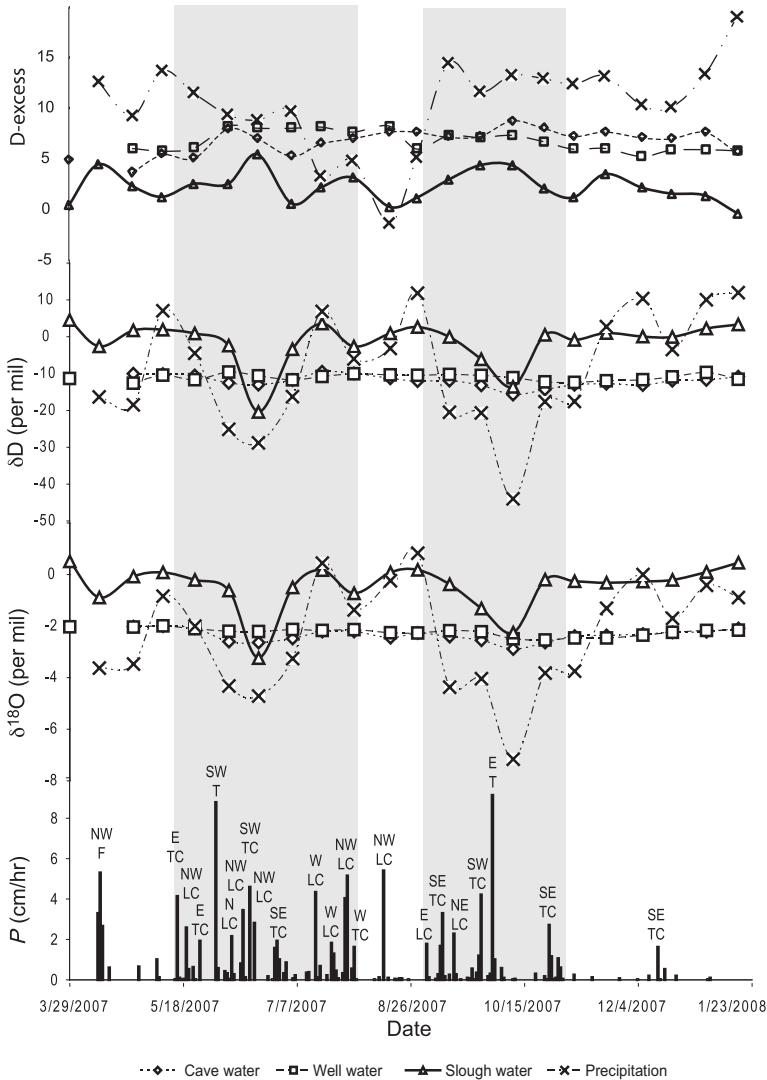


Figure 6. Compilation time-series plot of a hyetograph (P), ratios of stable isotopes ($\delta^{18}\text{O}$, δD), and D_{ex} . The size of the data marker is equal to or greater than the published precision of the instrumentation. Precipitation events that exceed a rate of 2 cm/h also include information about type and motion of the precipitation as indicated by Doppler radar (F – frontal, LC – local convection, TC – tropical convection, T – tropical system; N – north, NW – northwest, E – east, NE – northeast, S – south, SW – southwest, SE – southeast). Grey bars indicate the wet season.

Values of D_{ex} in the samples of precipitation have a distinct seasonal variation divided by the MSD in late-August (Figure 6). From the start of the study until the MSD, values of D_{ex} average 8.2 with a trend toward lower values and a minimum value of -1.25 on 8/17. After the MSD, values of D_{ex} remain consistently above 10 with an average of 13.1 and a maximum value of 19.1 on 1/16.

5. Discussion

The data from this study further resolve the degree of mixing between surface waters and shallow groundwater in the Everglades ecosystem and supplement the findings of Price and Swart [42]

during a study of similar scope. The differences between our respective studies are reflected in the geographic scale and data resolution. The study of Price and Swart was wider ranging and longer term. Forty-six wells and 23 surface-water sites were sampled over a more than 3000 km² region throughout the east-central Everglades between 1997 and 1999. Samples were collected on a monthly basis and many sites were not sampled during the course of the study. This study, in contrast, is much narrower in scale with a greater sampling frequency. All three sites are within an area of 5 km² and each site was sampled every two weeks.

Water-level changes are rapid, simultaneous, and of similar magnitude in both TS and Palma Vista Hammock (Figure 3). Precipitation is instantly manifested as an increase of water level either by direct addition to surface waters, as is the case for the slough, or by rapid percolation through a thin vadose zone of very porous and solution-modified rock, as is the case for the cave and the well (Figure 1b). In fact, on 12/06 at the cave, a 1 l application of water on the surface was heard dripping into the cave pool after only three minutes when the soil was dry and approximately 15 s after the soil was saturated. The water is likely being channelled via syndepositional [35] or root-generated macropores.

The water chemistry of the slough water also promptly changes following rainfall (Figure 5). For example, water in the slough experienced reduction of more than 100 μS in SpC in less than two hours during a major precipitation event on 10/1 (Figure 4). The same event reduced the SpC in the well by 15 μS . At broader time scales, the addition of rainwater during the rainy season oxygenates the water and dilutes the dissolved solids in the slough water, which in turn reduces the total alkalinity (Figures 3 and 5).

Compared to the geochemistry of the slough, the well and the cave exhibit less variance from dry season to wet season (Figures 3 and 5). One notable exception is the concentration of iron in the well; the rise in water level during the rainy season is concurrent with a sharp rise in the concentration of dissolved iron (Figure 5). The data suggests redox reactions as the phreatic surface migrates; however, principle component analysis by McGee *et al.* [46] supports the decomposition of iron-rich leaf matter during the wet season as the primary source of dissolved iron. The breakdown of this organic matter releases the less soluble Fe(III) bound to tannins and lignins, which flush through the vadose zone and convert to the more soluble Fe(II) in the reducing environment below the water table of the well (Figure 3). A plot of total and dissolved iron in the well (Figure 7) supports this hypothesis. Total iron increases rapidly to 342 $\mu\text{g/l}$ in the well at the onset of the wet season. Within two weeks, however, concentrations of total and dissolved iron are nearly equal, and remain similar through the rest of the wet season, indicating a complete conversion of the oxidised Fe(III) into the reduced Fe(II) (Figure 7).

Figure 5 also reveals that slough waters can have concentrations of Na and Mg elevated above the cave and well. Na in the slough, for example, averages 16 mg/l during winter and spring compared with an average of 7.2 mg/l in both the cave and the well (Figure 5). A similar pattern exists for Mg, with a dry season average in the slough of 4.5 and 1.7 mg/l in the cave and the well, respectively. Chloride, and to a lesser extent K, have the same annual pattern. The concentrations of Ca in the slough, while following the same trend as the other dissolved solids, have values in the dry season roughly equivalent to that of the cave and well and lower during the wet season (Figure 5). Simple concentration of surface waters due to ET and a mixing of surface water and one or more external sources such as precipitation, canal water, and deep groundwater may drive these observed patterns of dissolved solids in the slough compared to the cave and well. A second, less influential, factor could be cation exchange of the Ca on negatively charged clay particles in the soils within the agricultural areas north and east of the study area. The importance of evaporation in the slough compared with the cave and the well are clearly demonstrated by the precipitation-weighted mean values of δD and $\delta^{18}\text{O}$ in precipitation as presented in the results (Figure 6). Determining the relative proportions of external sources without concurrent end member comparisons is difficult.

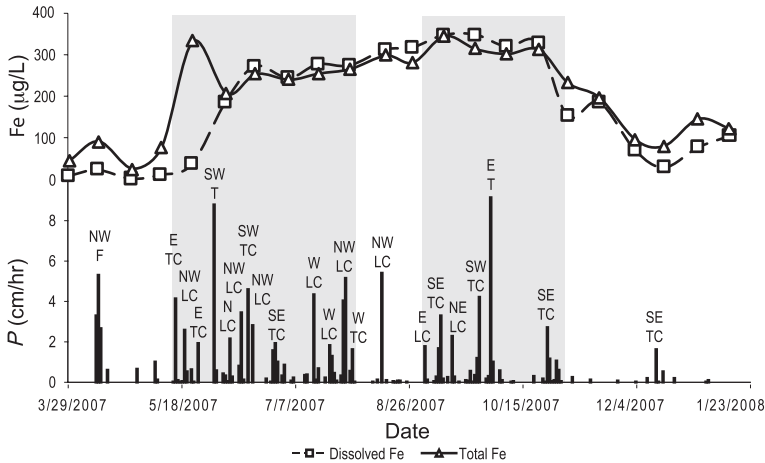


Figure 7. Plot of total and dissolved iron in the well in Palma Vista Hammock. The size of the data marker is equal to or greater than the published precision of the instrumentation. Precipitation events that exceed a rate of 2 cm/h also include information about type and motion of the precipitation as indicated by Doppler radar (F – frontal, LC – local convection, TC – tropical convection, T – tropical system; N – north, NW – northwest, E – east, NE – northeast, S – south, SW – southwest, SE – southeast). Grey bars indicate the wet season.

5.1. Moisture sources

A plot of δD versus $\delta^{18}O$ clearly reveals the effects of ET at our field site (Figure 8a). The local meteoric water line (LMWL) of precipitation samples in the Everglades $\delta D = 7.2(\delta^{18}O) + 8.6$ ($R^2 = 0.93$) is of similar character to the GMWL and closely conforms to the LMWL of $\delta D = 7.1(\delta^{18}O) + 9.9$ determined by Price and Swart [42]. Points on the LMWL cluster into two principle groups: (1) samples with a δD range of -6 to $+12$ ‰ and a $\delta^{18}O$ that ranges between -2 and $+1$ ‰ which are associated principally with local convection, and (2) samples with a δD range of -29 to -16 ‰ and $\delta^{18}O$ that ranges between -5 and -3 ‰ which are generally associated with tropical moisture or the passage of frontal systems (Figures 6 and 8a).

The time-series data of precipitation D_{ex} (Figure 6) further distinguish between moisture sources for precipitation. During the late spring and summer of 2007, and before the MSD, precipitation samples largely registered values of $D_{ex} < 10$ ‰. It is possible that these samples reflect continental moisture with a significant component provided by transpiration and carried by the Westerlies or moisture generated by local ET and convection. Samples with $D_{ex} > 10$ ‰ generally cluster in the fall and winter, after the MSD, and appear to be associated with evaporated maritime moisture carried along the Trade Winds. The pre-MSD data produce a regression of $\delta D = 6.6(\delta^{18}O) + 5.0$ compared to the post-MSD data, which produce a regression of $\delta D = 7.6(\delta^{18}O) + 11.3$ (Figure 8b). The t -test value comparing these D_{ex} data is 3.96, which is significant at the 95 % confidence interval. Full characterisation of the D_{ex} variation in the Everglades ecosystem values would require higher resolution sampling, as well as concurrent storm tracking information combined with land-use data.

A least squares fit using the samples from the well, the cave, and precipitation samples from tropical or frontal system produces a LEL with a slope of 5.6 and a R^2 of 0.97 (Figure 8a), an indication of significant evaporation [22]. The LEL fit demonstrates an additional, and important, point about Everglades hydrology. Samples from the slough are enriched in D and ^{18}O via ET along the LEL from shallow groundwater in the hammocks (the well and the cave). These waters in the hammocks themselves evolved along the LEL from tropical and frontal moisture sources, not localised convection. Whereas local convection is frequent, yet isolated and of short duration, tropical and frontal systems are infrequent, but widespread and long-lasting. Florea and Vacher

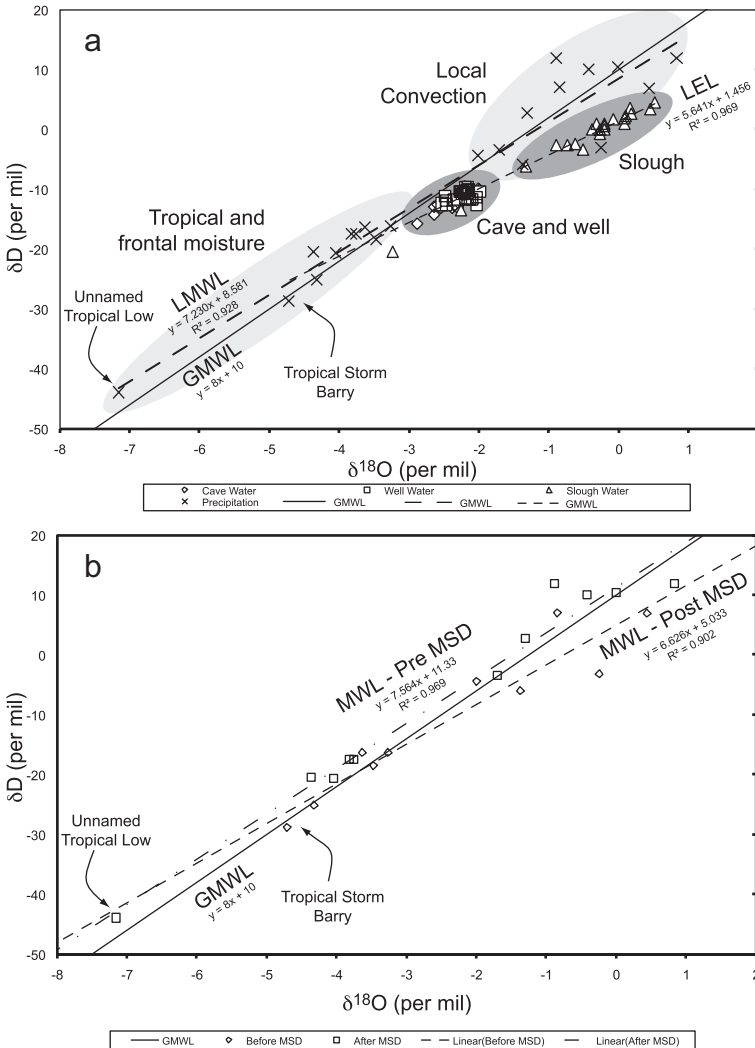


Figure 8. (a) Plot of δD versus $\delta^{18}O$ for samples of precipitation, surface water from the slough, and shallow groundwater from the cave and well. The size of the data marker is equal to or greater than the published precision of the instrumentation. The GMWL, LMWL, and LEL are shown along with regressions. The LEL connects samples from the slough, the cave, and the well to precipitation samples from frontal and tropical systems, which have a distinct isotopic signature from samples of precipitation that come from local convection. (b) Meteoric water line regressions through precipitation samples prior to and after the MSD.

[47] demonstrated the importance of tropical and frontal systems to aquifer recharge in west-central Florida. In the Everglades, tropical and frontal systems in the fall and spring, respectively, add new water to the flow system. Local convection recycles the available water, a statement supported by values of $D_{ex} < 10\%$ gathered during the parts of the wet season dominated by local convection (Figure 6). The regression of the pre-MSD D_{ex} data (Figure 8b), with a slope of 6.6, further supports the finding that land-based, evaporation-influenced source waters contribute to those samples of precipitation.

The data further illustrate that shallow groundwater in the hammocks and pine rocklands, depleted in D and ¹⁸O (Figure 6) evolves along the LEL towards surface water in the slough, which is enriched in the heavier isotopes. Mixing of surface water in the slough with shallow

groundwater in the hammocks appears limited. The limited geochemical changes in the cave and well compared to the slough (Figure 5) further illustrate this point. This finding parallels that of Price and Swart [42], who specifically demonstrated that the shallow groundwater in the pine rocklands recharges TS downstream of our field site. The evolution of waters along the LEL residence time of water in the hammock and in the slough is difficult to determine without the aid of concurrent tracer data.

5.2. Sources of dissolved solids

While δD and $\delta^{18}O$ data as well as those of Price and Swart [42] suggest that surface waters in TS evolve via ET alteration of shallow groundwater, our data regarding dissolved solids provide evidence that at least part of the surface waters in the study area have their source in the agricultural area to the north and east, outside of ENP. For example, the lowest concentrations of Na, Mg, K, and Cl in the slough are equivalent to the median value at the cave and well (13 mg/l for Cl – Figure 5). These low concentrations in the slough occur during the wet season, when frequent rains dilute the total dissolved solids (TDS). In contrast, elevated concentrations of these ions in the slough (27 mg/l for Cl) are the likely result of a combination of evaporation and source waters with higher original concentrations of these solutes. The EPA Region 4 and the South Florida Water Management District clearly states ‘the median concentration [of Cl in surface water during 2004–2005] in the refuge interior was 23 mg/l with a higher concentration in the marsh near the perimeter due to the penetration of mineral water from the surrounding canal’ [48, p. 37]. Our median Cl concentration is in exact agreement with this EPA data (Figure 5).

A graph of chloride versus sodium concentrations in the slough reveals a linear relationship, indicating an end-member mixing model between two water sources controlling the composition of the slough water (Figure 9a). Plots of mean values of chloride versus sodium for precipitation from the National Atmospheric Deposition Program, water from the well in Palma Vista Hammock, surface waters from the nearby C-111 Canal (USGS NWIS station ID 252414080333200), and shallow groundwater samples from a depth of 25 m in the G-3319B well near the L-31W Canal [42] (Figures 1a and 9b), illustrate that precipitation and the shallow groundwater north of the study area are the likely end members. Projecting the paired sodium-chloride data onto the regression through the data provide a tool to compute the relative proportion of the sample explained by the shallow groundwater (Figure 9b).

Shallow groundwater near the L-31W Canal explains between 18 and 69 % of the slough water (Figure 9b) with the percent composition linked to the magnitude of precipitation during the sampling period (Figure 5). In contrast, shallow groundwater near the L-31W Canal explains only one-quarter of the composition of the water in the well. Price and Swart [42] propose that this level of chloride in the pine rocklands may represent atmospheric deposition of sea spray with a computed recharge rate between 8 and 12 cm/year. Finally, the lower average values of TDS in the cave and the well (Figure 5) point towards less influence by evaporation; a point illustrated by (1) the lower average temperature and higher average RH readings in the hammock (Figure 2b), and (2) the fact that evaporation is greatly reduced in shallow groundwater compared with surface water.

In the slough, the highest values of SO_4 , K, and NO_3 occur on 4/11, which immediately follows the first major rainfall of the year (Figure 5). Following Orem [49], we attribute the SO_4 to runoff of agricultural sulphur used as soil amendment throughout the year in the agricultural areas to the north and east of ENP. For comparison, sulphates contamination entering ENP from the L-67 canal has been documented to the north of the study area (Figure 1a) [48]. In our study, the sulphates may enter TS via the S-322 pump station on the L-31W canal 3 km to the

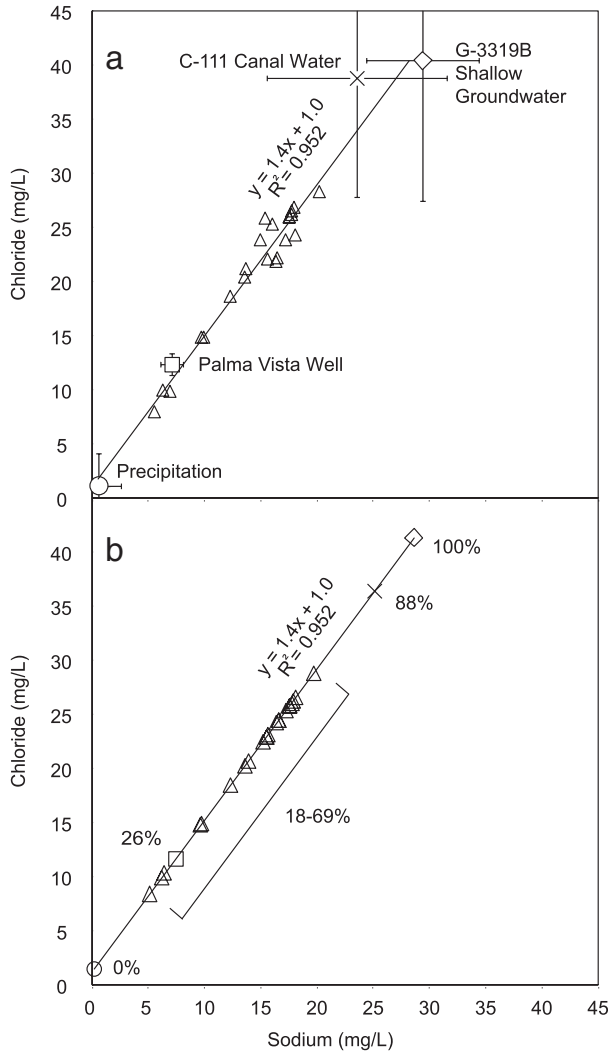


Figure 9. (a) Plot and regression line through chloride versus sodium concentration data for the slough water, the mean value for the Palma Vista Well, the mean values for precipitation from the National Atmospheric Deposition Program and shallow groundwater in the G-3319B well [42], and the mean value of surface water in the C-111 canal between 1995 and 2004 (NWIS station ID 252414080333200). (b) Linear mixing model between precipitation and shallow groundwater using data projected onto the regression line. Percentages are the portion of the sample that is similar to the value of shallow groundwater.

northeast of the sampling site (Figure 1a) and concentrate as elemental sulphur in a reduced form in the soils of TS. During the dry season, soil oxidation converts this reduced sulphur to sulphur [50,51]. At the end of the dry season, the first major precipitation event in the Everglades liberates the SO_4 during soil rewetting [49]. This process of accumulation during the dry season and liberation at the onset of the wet season could similarly explain the spikes in both K and NO_3 on 4/11.

Collectively, the TDS data, the ion chemistry, and the mixing model support the isotope data that demonstrate that the direction of shallow groundwater flow is from Palma Vista Hammock and the pine rocklands to TS. Furthermore, these data clearly establish that source waters, particularly shallow groundwater, to the north and east of ENP influence the geochemistry in TS.

This information, in combination with the climatologic implications of the stable isotope data, may have broader implications to the management of water resources in the south Florida ecosystem.

6. Conclusions

The data from this study reveal a dynamic geochemical environment in the surface water of ENP that is very sensitive to dilution from rainfall and input from external sources, chiefly shallow groundwater to the north and east of ENP. Shallow groundwater in the hammocks and pine rocklands, on the other hand, remains geochemically stable during the year. Of particular influence to the geochemistry of surface waters are large-scale, external sources of moisture such as tropical systems in the late summer and fall, and occasional frontal systems in the late winter and spring. The input of surface water from canals, specifically the L-31W canal, is also evident in a linear mixing model between precipitation and shallow groundwater near the L-31W canal and the data for TDS, particularly SO_4 , K, and NO_3 that are associated with agricultural areas to the north and east of ENP.

Stable isotopes of hydrogen and oxygen in samples of precipitation fit to a LMWL of $\delta\text{D} = 7.2(\delta^{18}\text{O}) + 8.6$ ($R^2 = 0.93$) with a similar slope and intercept to the GMWL. These samples clearly subdivide into two groups representing types of precipitation, those less depleted in the heavier isotope that represent local convection and those strongly depleted in the heavier isotope derived from tropical cyclones or frontal systems. The LEL that passes through the δD and $\delta^{18}\text{O}$ data from the cave, the well, and the slough gives an equation of $\delta\text{D} = 5.6(\delta^{18}\text{O}) + 1.5$ ($R^2 = 0.97$) and intersects the LMWL at the isotopic signature of tropical cyclones or frontal systems. This implies that shallow ground water and surface water in the ENP evolve along the LEL from tropical or frontal systems and not local convection.

Values of D_{ex} during the study combined with wind and radar data reveal two principle sources of atmospheric moisture separated by the MSD during mid- to late-August. While our measurements are prone to some degree of error, the first set are samples with $D_{\text{ex}} < 10$ in late spring and early summer that generally indicate mixed air masses that include frontal systems conveyed by the Westerlies and summertime local convection that represent continental moisture influenced by transpiration. The second set are samples with $D_{\text{ex}} > 10$ in the late summer and fall that likely represent moisture derived from evaporated maritime sources, such as tropical systems, brought onshore by the Trade Winds.

Acknowledgements

Research in ENP occurred under Park Service permit number EVER-2007-SCI-0020 issued to the US Geological Survey. Funds provided as part of a USGS Mendenhall Postdoctoral Fellowship to Florea paid for sample collection and analysis. The authors are grateful for engaging discussions and mentorship with Kevin Cunningham, Peter Harries, Jonathan Wynn, Bogdan Onac, and Jason Polk, as well as the constructive comments of two anonymous reviewers.

References

- [1] I. Clark and P. Fritz, *Environmental Isotopes in Hydrogeology* (Lewis Publishers, Boca Raton, 1997).
- [2] C. Kendall and T.B. Coplen, Distribution of Oxygen-18 and Deuterium in River Waters Across the United States, *Hydrol. Process.* **15**, 1363 (2001).
- [3] W. Dansgaard, Stable Isotopes in Precipitation, *Tellus* **16**, 436 (1964).
- [4] B.G. Katz, *Using $\delta^{18}\text{O}$ and δD to Quantify Ground-Water/Surface-Water Interactions in Karst systems in Florida*, paper presented at the *National Water Quality Monitoring Council Conference*, Natl. Water Quality Monit. Council., Reno, Nev., 1998.
- [5] H. Craig, Isotopic Variations in Meteoric Waters, *Science* **133**, 1702 (1961).

- [6] E.R. Cook, R.D. D'Arrigo, and M.E. Mann, A Well-Verified, Multiproxy Reconstruction of the Winter North Atlantic Oscillation Index Since A. D. 1400, *J. Clim.* **15**, 1754 (2002).
- [7] R. D'Arrigo, E.R. Cook, R.J. Wilson, R. Allan, and M.E. Mann, On the Variability of ENSO Over the Past Six Centuries, *Geophys. Res. Lett.* **32**, L03711 (2005), doi: 10.1029/2004GL022055.
- [8] D.W. Gamble, Water Resource Development on Small Carbonate Islands: Solutions Offered by the Hydrologic Landscape Concept, in *WorldMinds: Geographic Perspectives on 100 Problems*, edited by D.G. Janelle, B. Warf, and K. Hansen (Kluwer Academic Publishers, Dordrecht, The Netherlands, 2004), pp. 503–508.
- [9] R.A. Renken, J. Dixon, J. Koehmstedt, S. Ishman, A.C. Lietz, R.L. Marella, P. Telis, J. Rogers, and S. Memberg, Impact of Anthropogenic Development on Coastal Groundwater Hydrology in Southeastern Florida, 1900–2000, USGS Circular 1275, 2005.
- [10] G.C. Borotolami, B. Ricci, G.F. Susella, and G.M. Zuppi, Isotope Hydrology of the Val Corsaglia, Maritime Alps, Piedmont, Italy, in *Isotope Hydrology* (IAEA Symposium, 1979), Vol. 228, pp. 327–350.
- [11] M. Yurtsever and J.R. Gat, Stable Isotope Hydrology: Deuterium and Oxygen-18 in the Water Cycle, in *Atmospheric Waters* (IAEA TRS-210, 1981), pp. 103–142.
- [12] K. Rozanski, L. Araguas-Araguas, and R. Gonfiantini, Isotopic Patterns in Modern Global Precipitation, in *Climate Change in Continental Isotopic Record*, edited by P.K. Swart, K.C. Lohmann, and J. McKenzie (American Geophysical Union, Geophysical Monograph Series, 1993), Vol. 78, pp. 1–36.
- [13] N. Ingraham, Isotopic Variations in Precipitation, in *Isotopic Tracers in Catchment Hydrology*, edited by C. Kendall and J.J. McDonnell (Elsevier, Amsterdam, 1998), pp. 87–188.
- [14] P. Gremillion and M. Wanielist, Effects of Evaporative Enrichment on the Stable Isotope Hydrology of Central Florida (USA), *River Hydrol. Process.* **14**, 1465 (2000).
- [15] L. Araguas-Araguas, K. Froehlich, and K. Rozanski, Deuterium and Oxygen-18 Isotope Composition of Precipitation and Atmospheric Moisture, *Hydrol. Process.* **14**, 1341 (2000).
- [16] H.C. Fricke and J.R. O'Neil, The Correlation Between 18O/16O Ratios of Meteoric Water and Surface Temperature; its Use in Investigating Terrestrial Climate Change Over Geologic Time, *Earth Planet. Sci. Lett.* **170**, 181 (1999).
- [17] L. Merlivat and J. Jouzel, Global Interpretation of the Deuterium-Oxygen 18 Relationship for Precipitation, *J. Geophys. Res.* **84**, 5029 (1979).
- [18] K.J. Cunningham, M.A. Wacker, E. Robinson, C.J. Gefvert, and S.L. Krupa, Hydrogeology and ground-water flow at Levee 31N, Miami-Dade County, Florida, July 2003 to May 2004. U.S. Geological Survey Scientific Investigations Map I-2846 (2004).
- [19] E. Salati, A. Dall'Olio, J.R. Gat, and E. Matsui, Recycling of Water in the Amazon Basin: An Isotopic Study. *Water Resour. Res.* **15**, 1250 (1979).
- [20] L.A. Martinelli, R.L. Victoria, L.S.L. Sternberg, A. Ribeiro, and M.Z. Moreira, Using Stable Isotopes to Determine Sources of Evaporated Water to the Atmosphere in the Amazon Basin, *J. Hydrol.* **183**, 191 (1996).
- [21] Z. Liu, L. Tian, T. Yao, and W. Yu, Seasonal Deuterium Excess in Nagqu Precipitation: Influence of Moisture Transport and Recycling in the Middle of Tibetan Plateau, *Environ. Geol.* **55**, 1501 (2008).
- [22] F. Gonfiantini, Environmental Isotopes in Lake Studies, in *Handbook of Environmental Isotopes Geochemistry*, edited by P. Fritz and J.-Ch. Fontes (Elsevier, Amsterdam, 1986), Vol. 2, pp. 113–168.
- [23] G.D. Farquhar, L.A. Cernusak, and B. Barnes, Heavy Water Fractionation During Transpiration, *Plant Physiol.* **143**, 11–18 (2007).
- [24] M.C. Peel, B.L. Finlayson, and T.A. McMahon, Updated World Map of the Köppen-Geiger Climate Classification, *Hydrol. Earth Syst. Sci.* **11**, 1633 (2007).
- [25] E. Aguado and J.E. Burt, *Understanding Weather and Climate*, 3rd ed. (Pearson Education, Upper Saddle River, NJ, 2004).
- [26] M. Kottek, J. Grieser, C. Beck, B. Rudlof, and F. Rubel, World Map of Köppen-Geiger Climate Classification Updated, *Meteorol. Zeit.* **15**, 259 (2006).
- [27] S. Hastenrath, Rainfall Distribution and Regime in Central America. *Arch. Meteorol. Geophys. Bioklimatol., Ser. B* **15**, 201 (1967).
- [28] A.A. Chen and M.A. Taylor, Investigating the Link Between Early Season Caribbean Rainfall and the El Niño 1 Year, *Int. J. Climatol.* **22**, 87 (2002).
- [29] S. Curtis, Interannual Variability of the Bimodal Distribution of Summertime Rainfall Over Central America and Tropical Storm Activity in the Far-Eastern Pacific, *Clim. Res.* **22**, 141 (2002).
- [30] V. Magaña, J.A. Amador, and S. Medina, The Midsummer Drought Over Mexico and Central America, *J. Clim.* **12**, 1577 (1999).
- [31] A. Giannini, Y. Kushnir, and M.A. Cane, Interannual Variability of Caribbean Rainfall, ENSO, and the Atlantic Ocean, *J. Clim.* **13**, 297 (2000).
- [32] S. Hastenrath, The Intertropical Convergence Zone of the Eastern Pacific Revisited, *Int. J. Climatol.* **22**, 347 (2002).
- [33] S. Curtis and D. Gamble, Regional Variations of the Caribbean Mid-Summer Drought, *Theor. Appl. Climatol.* **94**, 25 (2008).
- [34] D.W. Gamble, D.B. Parnell, and S. Curtis, Spatial Variability of the Caribbean Midsummer Drought and Relation to the North Atlantic High, *Int. J. Climatol.* **28**, 343 (2008).
- [35] K.J. Cunningham, M.C. Sukop, H. Huang, P.F. Alvarez, H.A. Curran, R.A. Renken, and J.F. Dixon, Prominence of Ichnologically Influenced Macroporosity in the Karst Biscayne Aquifer: Stratiform 'Super-K' Zones, *Geol. Soc. Am. Bull.* **121**, 164 (2009).

- [36] L.J. Florea and A.J. Yuellig, Everglades National Park – Surveying the Southernmost Cave in the Continental United States, *Inside Earth* **10**, 3 (2007).
- [37] K.J. Cunningham and L.J. Florea, The Biscayne Aquifer in Southeast Florida, in *Caves and Karst of America*, edited by A. Palmer and M.V. Palmer (National Speleological Society, Huntsville, Alabama, 2009), pp. 196–199.
- [38] J.E. Mylroie, J.L. Carew, and H.L. Vacher, Karst Development in the Bahamas and Bermuda, in *Terrestrial and Shallow Marine Geology of the Bahamas and Bermuda*, *Geological Society of America Special Paper 300*, edited by H.A. Curran and B. White (Geological Society of America, Boulder, Colorado, 1995), pp. 251–267.
- [39] J.W. Harvey, S.L. Krupa, and J.M. Krest, Ground Water Recharge and Discharge in the Central Everglades, *Ground Water* **42**, 1090 (2004).
- [40] J.G. Meyers, P.K. Swart, and J.L. Meyers, Geochemical Evidence for Groundwater Behavior in an Unconfined Aquifer, South Florida. *J. Hydrol.* **148**, 249 (1993).
- [41] W. Wilcox, Use of Stable Isotopes to Quantify Flows Between the Everglades and Urban Areas in Miami-Dade County Florida, *J. Hydrol.* **293**, 1 (2004).
- [42] R.M. Price and P.K. Swart, Geochemical Indicators of Groundwater Recharge in the Surficial Aquifer System, Everglades National Park, Florida, USA, in *Perspectives on Karst Geomorphology, Hydrology, and Geochemistry – A Tribute to Derek C. Ford and William B. White*, *Geological Society of America Special Paper 404*, edited by R.S. Harmon and C. Wicks (Geological Society of America, Boulder, Colorado, 2006), pp. 251–266.
- [43] C.L. Jordan, Florida's Weather and Climate: Implications for Water, in *Water Resources Atlas of Florida*, edited by E.A. Fernald and D.J. Patton (Institute of Science and Public Affairs, Florida State University, 1984), pp. 18–35.
- [44] E.R. German, Regional Evaluation of Evapotranspiration Rates in the Everglades, U.S. Geological Survey, Water-Resource Investigations Report 00-4217, 2002, p. 48.
- [45] B.P. Onac, K. Pace-Graczyk, and V. Atudireic, Stable Isotope Study of Precipitation and Cave Drip Water in Florida (USA): Implications for Speleothem-Based Paleoclimate Studies, *Isot. Environ. Health Stud.* **44**, 149 (2008).
- [46] D.K. McGee, J.G. Wynn, L.J. Florea, and P.J. Harries, *In Review. Characterizing Biologically-Driven Limestone Dissolution Mechanisms in a Modern Tropical Wetland* (Everglades National Park, USA).
- [47] L.J. Florea and H.L. Vacher, Hydrology of Eogenetic Karst Illustrated by the 2004 Hurricanes, Florida, *Ground Water* **45**, 439 (2007).
- [48] D.J. Scheidt and P.I. Kalla, Everglades Ecosystem Assessment: Water Management and Quality, Eutrophication, Mercury Contamination, Soils and Habitat: Monitoring for Adaptive Management: A R-EMAP Status Report, USEPA Region 4, Athens, GA, EPA 904-R-07-001, 2007, p. 98.
- [49] W.H. Orem, Sulfur Contamination in the Florida Everglades: Initial Examination of Mitigation Strategies: U.S. Geological Survey Open-File Report 2007-1374, 2007.
- [50] D.P. Krabbenhoft and L. Fink, The Effect of Dry Down and Natural Fires on Mercury Methylation in the Florida Everglades, *2001 Everglades Consolidated Report, Appendix 7-8*, South Florida Water Management District, 2001, p. 14.
- [51] C.C. Gilmour, D.P. Krabbenhoft, W. Orem, and G. Aiken, Influence of Drying and Rewetting on Mercury and Sulfur Cycling in Everglades and STA Soils, *2004 Everglades Consolidated Report. Appendix 2B-1*, South Florida Water Management District, 2004, p. 19.